ARCHIVE

O F

MECHANICAL

ENGINEERING

DOI: 10.24425/ame.2025.154744

2025, Vol. 72, No. 3, pp. 473-484



Analysis of the influence of the heat transfer model on the effectiveness of the heat exchanger on the example of cross flow device

Received 26 June 2025, Revised 4 August 2025, Accepted 15 August 2025, Published online 23 August 2025

Keywords: cross flow heat exchanger, heat transfer effectiveness, forced convection, Nusselt number

One of the methods of analyzing a heat exchanger consists in determining the heat transfer rates and outlet temperatures of the fluids for known mass flows, inlet temperatures, and exchanger type and size. This requires calculating the exchanger performance for known transfer surface area but unknown outlet temperatures. The concept of the heat transfer effectiveness (HTE) can be applied to determine the heat transfer rate of the specified heat exchanger without knowing the outlet temperatures of the fluids. This article presents the results of calculations of the HTE parameter for a cross-flow heat exchanger with staggered tube banks. The analysis takes into account six different models of convection heat transfer over the tube banks. In this scenario, the impact of the applied convection model on the value of HTE for the considered heat exchanger was examined. For the considered calculation cases, the value of the HTE parameter is in the range from 0.3 to 0.48 and it decreases with the increase of the flow rate of both air and the flue gases. It has been shown that the results of all four models are very similar, while the other two models bring about either an increase or a decrease of the values of the parameter investigated. It was found that for the analyzed heat exchanger a simplified criterion for the convection heat transfer over tube banks can be used to determine the effectiveness of the heat transfer with the Reynolds number being the only parameter.

⁴Faculty of Power and Aeronautical Engineering, Institute of Aeronautics and Applied Mechanics, Warsaw University of Technology, Warsaw, Poland



Mariusz SALWIN, e-mail: mariusz.salwin@pw.edu.pl

¹Faculty of Production Engineering and Materials Technology, Czestochowa University of Technology, Częstochowa, Poland

²Faculty of Mechanical and Industrial Engineering, Institute of Organization of Production Systems, Warsaw University of Technology, Warsaw, Poland

³Faculty of Mechanical and Industrial Engineering, Institute of Manufacturing Technology, Warsaw University of Technology, Warsaw, Poland



1. Introduction

Heat exchangers play an essential role in different industrial and technical processes related to thermal energy management [1–4]. Efficient heat exchangers are needed to develop new energy-efficient technologies to decrease energy consumption [5–8]. Therefore, the scientists focus their efforts on improving the design of devices as well as improving the thermal properties of working fluids [9–12]. Energy savings can be achieved by improving the performance of the heat exchangers [13–16]. One way to achieve this goal is analytical modelling of their construction [17–20].

For the analytical modeling of the heat exchangers one of the following two methods, i.e., either the log mean temperature difference (LMTD) or the effectiveness-NTU is most often used. The LMTD method is applied when the inlet and outlet temperatures of the hot and cold fluids are known or can be determined from the energy balance, while the effectiveness-NTU method is used for the determination of the heat transfer rate and the fluid outlet temperatures in the case the fluid mass flow rates and inlet temperatures are known and the construction of heat exchanger is specified. The NTU method is based on a dimensionless parameter called the heat transfer effectiveness, HTE, defined as [21–23]:

$$HTE = \frac{Q}{Q_{\text{max}}}, \tag{1}$$

where Q is the actual heat transfer rate, and Q_{max} is the maximum possible heat transfer rate in a heat exchanger.

The effectiveness of a heat exchanger is a function of a dimensionless quantity called the number of transfer units NTU. This parameter is defined as [24]:

$$NTU = \frac{U A_s}{C_{\min}} = \frac{U A_s}{(\dot{m} c_p)_{\min}},$$
 (2)

where: U is the overall heat transfer coefficient, A_s is the heat transfer surface area of the analyzed heat exchanger and C_{\min} is the smaller heat capacity rate of the cold and hot fluids. The effectiveness relations have been developed for several types of heat exchangers. For the single-pass cross-flow heat exchanger, that parameter may be expressed as [25]:

HTE =
$$\frac{1}{c} (1 - \exp(1 - c(1 - \exp(-NTU)))),$$
 (3)

where c is the capacity ratio defined as:

$$c = \frac{C_{\min}}{C_{\max}}.$$
 (4)

The original aim of the presented analyses was to demonstrate the impact of the adopted forced convection model for a staggered tube bunks on the heat transfer Analysis of the influence of the heat transfer model on the effectiveness of the heat...

effectiveness (HTE) results for the NTU method. A total of six different models were analyzed. The results obtained showed that four of the models were very similar. However, two other models produced results that differed by a few percent. One of these models underestimated the results, and the other one overestimated them.

2. Analysis and modelling

From equations (2) and (3), it may be concluded that the HTE parameter depends on the value of the coefficient U. In the case when the heat flow in the exchanger runs through a cylindrical baffle, the value of the coefficient U may be calculated from equation [26]:

$$U = \left(\frac{r_o}{r_i h_i} + \frac{r_o}{k} \ln \frac{r_o}{r_i} + \frac{1}{h_o}\right),\tag{5}$$

where: r_o , r_i – outer and inner radius of the tube, k – thermal conductivity of the tube, h_o , h_i – heat transfer coefficients on the outer and inner surfaces of the tube. The coefficients h_o and h_i may be calculated as:

$$h_i = \frac{\text{Nu}_i \, k_i}{d_i} \,, \tag{6a}$$

$$h_o = \frac{\text{Nu}_o \, k_o}{d_o} \,, \tag{6b}$$

where d_o , d_i are the outer and inner diameters of the tube, while k_i and k_o are thermal conductivities of the fluids. The Nusselt numbers in equations (6) are determined from the corresponding criterial equations, while for the calculation of the Nu_i number the equation for a forced convection in a straight circular channel should be used [27]:

$$Nu_i = 0.023 \,\text{Re}_i^{0.8} \,\text{Pr}_i^{0.4}. \tag{7}$$

In order to calculate the Nu_o number, the equations for the opposing flow convection through the tube banks should be used [28]:

$$Nu_o = C \operatorname{Re}_o^A \operatorname{Pr}_o^B. \tag{8}$$

The values of the C, A, and B coefficients from the equation (8) are selected depending on the heat transfer case and are characterized by the Reynolds number and the geometry of the heat exchange system.

In a heat exchanger that contains a tube bank, the tubes are usually arranged either in-line or staggered ahead of the flow direction. In the current paper, the heat exchanger with a staggered arrangement is investigated and its geometry is characterized by three pitches between the tube centers, i.e., the transverse pitch X_t , the longitudinal pitch X_l and the diagonal pitch X_d (Fig. 1).

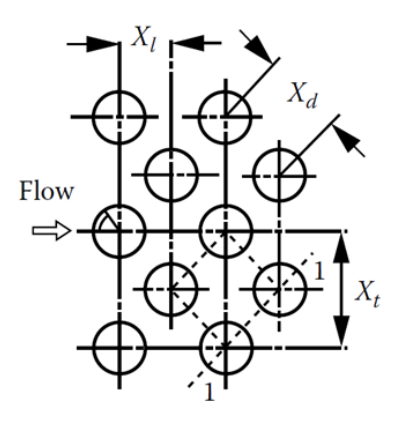


Fig. 1. Tube arrangement in a staggered tube bank design

Before presenting the details of relationships for the calculation of the Nusselt number, Nu_o , it is necessary to define the conditions under which the model calculations are carried out.

It is assumed that the heat exchanger consists of one tube bundle located inside a rectangular flue gas duct (Fig. 2). The heated medium is air that is flowing inside the tubes (pipes). The heating medium is the flue gas from the combustion of the natural gas. The heating medium flows outside the heat exchanger tubes. The discussed system is characterized by the geometric parameters, which are summarized in Table 1.

		-
Parameter	Parameter symbol	Value
width of the flue gas duct	l_x	0.75 m
height of the flue gas duct	l_w	0.55 m
tube outer diameter	d_o	31.8 mm
tube inner diameter	d_i	28.6 mm
tube rows number	n_{x}	10
number of tubes in an odd row	n_w	12
number of tubes in an even row	$(n_w - 1)$	11
transverse pitch	X_t	0.0442 m
longitudinal pitch	X_l	0.0442 m
diagonal pitch	X_d	0.0494 m
tubes total number	n_t	115
total flow area inside the tubes	A_i	0.0738 m^2
heat transfer area	A_s	8.61 m ²

Table 1. The geometric parameters of the discussed heat exchanger



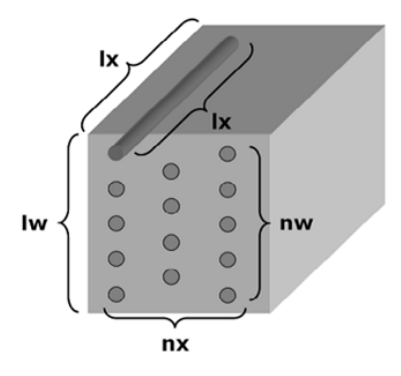


Fig. 2. The geometry of the analyzed heat exchanger

As it comes out from equations (6)–(8), the heat transfer coefficients h_i and h_o depend on the Reynolds numbers and are affected by the flow structure in the exchanger. The values of Reynolds numbers for air (Re_i) and the flue gas (Re_o) are summarized in Table 2 for some selected flow velocities, w. For the range of Re_o values shown in Table 2, several detailed correlations for the Nusselt number or for the coefficient h for cross flow over staggered tube banks can be found in the literature.

w, m/s	Re_o	Re_i
2	3358	1781
6	10075	5343
10	16792	8904
14	23509	12466
18	30226	16028
22	36943	19590
26	43659	23151
30	50376	26713

Table 2. Reynolds numbers for air and the flue gas for some chosen flow velocities, w

When performing the calculations, the velocity of the air and the flue gas was varied independently between 2 m/s and 28 m/s. It was also assumed that the inlet temperatures of the air and the flue gas were constant and set up at 20°C and 650°C, respectively. The data necessary for the calculations of the thermal properties of the fluids (i.e., its thermal conductivity, specific heat, dynamic viscosity and Prandtl number) were taken from the literature [29, 30], while the average densities were calculated according to the Clapeyron equation.

The calculation results presented and discussed in the current paper were obtained with the use of the following six correlations (models):

Model 1 (M1) [23]

$$Nu_o = 0.41 \operatorname{Re}_o^{0.6} \operatorname{Pr}_o^{0.33} \left(\frac{\operatorname{Pr}_o}{\operatorname{Pr}_w} \right)^{0.25}, \tag{9}$$

where: Pr_o and Pr_w are the Prandtl numbers calculated for average temperatures of the flue gas and the tube surface.

Model 2 (M2) [31]

$$Nu_o = 0.4 \operatorname{Re}_o^{0.6} \operatorname{Pr}_o^{0.36} \left(\frac{\operatorname{Pr}_o}{\operatorname{Pr}_w} \right)^{0.25}. \tag{10}$$

Model 3 (M3) [30]

$$Nu_o = F \cdot 0.35 \left(\frac{X_t}{X_l}\right)^{0.2} Re_o^{0.6} Pr_o^{0.36} \left(\frac{Pr_o}{Pr_w}\right)^{0.25}.$$
 (11)

where F is a correction factor, for $n_x = 10$, F = 0.98.

Model 4 (M4) [28]

$$Nu_o = \left(0.437 + 0.587 \,\text{Re}_o^{0.52}\right) \text{Pr}_o^{0.3} \,. \tag{12}$$

Model 5 (M5) [28]

$$h_o = f_a \,\varphi_p \frac{w_{o,\text{max}}^{0.61}}{d_o^{0.39}},\tag{13}$$

where: $w_{o,\text{max}}$ is the flue gas velocity at the minimum cross-section at the standard conditions and:

$$f_a = 0.874 + \frac{0.286}{\left(\frac{X_t}{d_o}\right)^2} + 0.84 \frac{X_t}{d_o},$$
 (14)

$$\varphi_p = 1.74\sqrt[4]{T_o}\,,\tag{15}$$

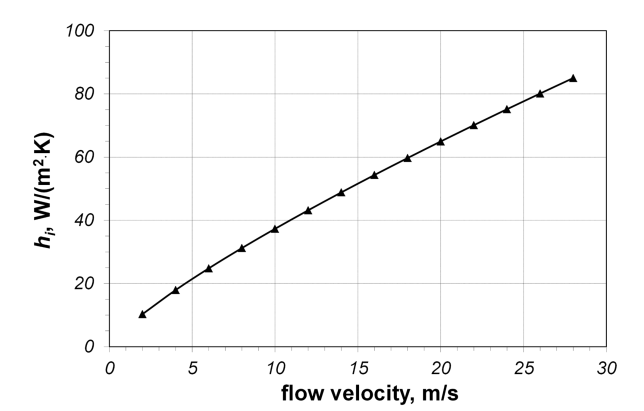
where T_o is the average absolute temperature of the flue gas.

Model 6 (M6) [27]

$$Nu_o = 0.37 \, Re_o^{0.6} \,. \tag{16}$$

3. Results and discussion

The data of the heat transfer coefficients for air h_i and waste gas h_o are presented in Figs. 3 and 4, respectively. For the considered range of the air velocities, the value of the coefficient h_i increases almost linearly from roughly 10.3 W/(m² K) to 85.1 W/(m² K).



Analysis of the influence of the heat transfer model on the effectiveness of the heat . . .

Fig. 3. Heat transfer coefficient for air h_i versus the flow velocity

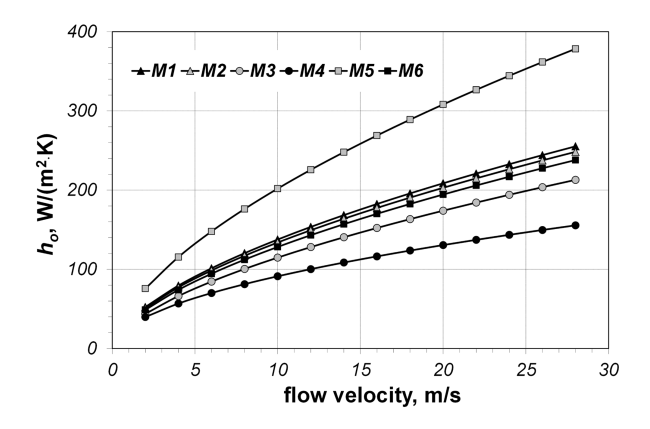


Fig. 4. Heat transfer coefficient for the flue gas h_o vs. the flow velocity and the model considered

The values obtained for the coefficient h_o depend on the individual models applied. The most similar are the results of the models M1, M2 and M6, which differ maximally by only 7.3%. The highest values are obtained for the model M5 and, compared with the model M6, the results vary by more than 55–60% (depending on the flow velocity). However, compared with M6, the results of the models M3 and M4 are underestimated by roughly 10.5% and 18.6–34.6%, respectively. Thus, the choice of the criterion equation for the convection over a chosen tube bank is crucial for the calculated values of the heat transfer coefficient, h_o .

The values of the HTE parameter that are obtained for the considered calculation cases are presented in Figs. 5–9. The individual figures refer to the results obtained for various air velocities (4, 10, 16, 22, and 28 m/s, respectively). In each figure, the results for all the models considered are shown for the assumed flue gas velocities of from 2 m/s to 26 m/s.

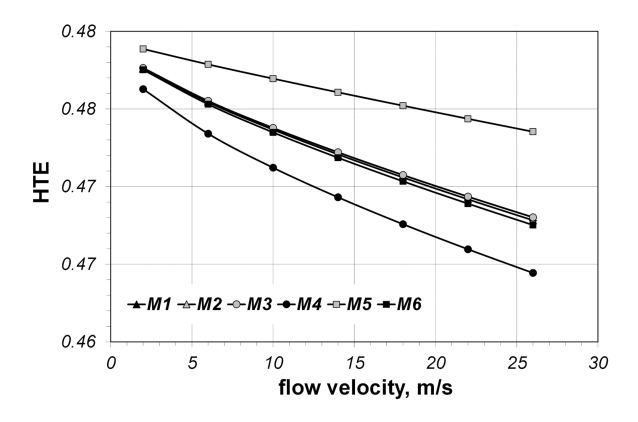


Fig. 5. Heat transfer coefficient values obtained for air velocity $w_i = 4$ m/s

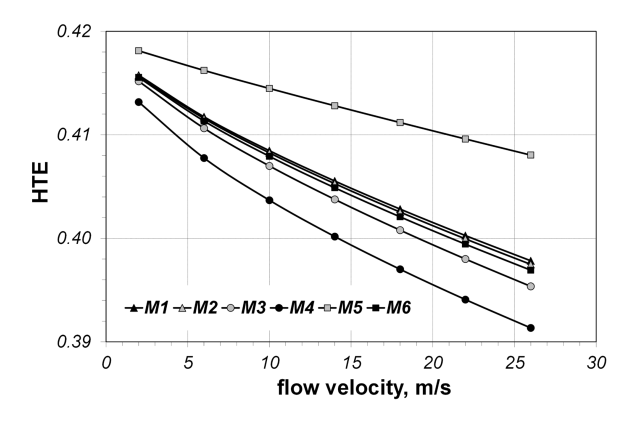


Fig. 6. Heat transfer coefficient values obtained for air velocity $w_i = 10$ m/s

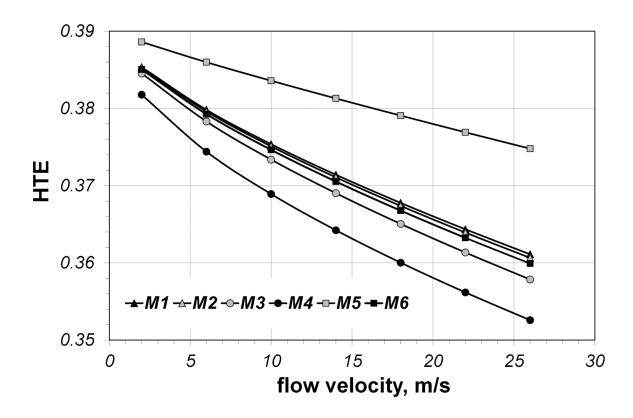


Fig. 7. Heat transfer coefficient values obtained for air velocity $w_i = 16$ m/s

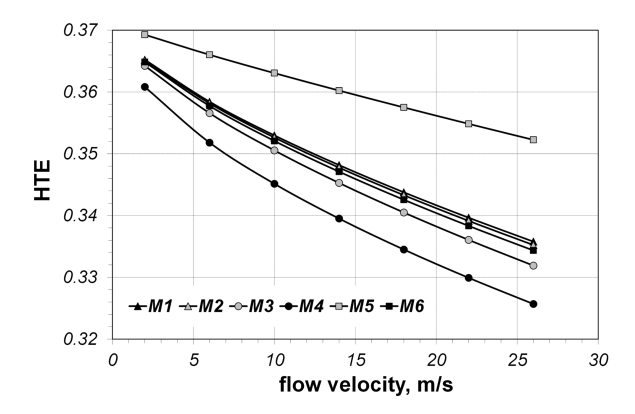


Fig. 8. Heat transfer coefficient values obtained for air velocity $w_i = 22 \text{ m/s}$

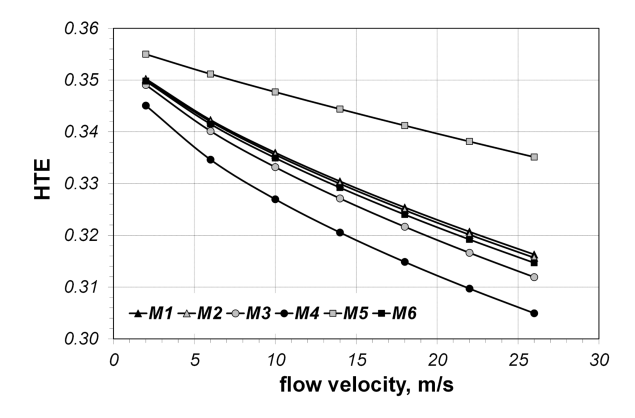


Fig. 9. Heat transfer coefficient values obtained for air velocity $w_i = 28 \text{ m/s}$

Generally, the value of the HTE parameter varies from 0.3 to 0.47. As it may be seen, the increase in the air or flue gas velocity brings about the reduction of the HTE value. This effect may seem quite surprising because generally, an increase in flow velocity causes an increase in the intensity of heat transfer in the heat exchanger. However, the changes of the flow velocity also affect the capacity ratio c, on which the HTE parameter also depends (cf. equation (3)). The problem will not be discussed further in this paper since the explanation of the phenomena goes beyond the scope of the current analysis. It is important, however, to investigate and present the influence of the adopted convection model on the obtained values of the HTE. From the analysis of the results shown in Figs. 5–8, it may be concluded that the extreme values of the HTE parameter were obtained for the M4 (HTM_{min}) and M5 (HTM_{max}) models. These models are quite different from the other ones, since the model M4 assumes a non-linear (logarithmic) relationship. For the majority of other models, that relationship can be written as [28]:

$$\log Nu_o = \log D + A \log Re_o, \tag{17}$$

$$\log \text{Nu}_o = \log H + B \log \text{Pr}_o. \tag{18}$$

The difference between the M5 and other models is even greater since the criterion numbers are not used in it and the coefficient h_o is described directly. For a more precise analysis, the maximum difference of the HTE values was calculated according to the following relationship:

$$\Delta HTE = \frac{HTE_{M5} - HTE_{M4}}{HTE_{M4}} \cdot 100\%. \tag{19}$$

where HTE_{M4}, HTE_{M5} are the values of the HTE parameter for the models M4 (HTM_{min}) and M5 (HTM_{max}), respectively. The changes of the values of Δ HTE for some selected values of the air velocities w_i as a function of the flue gas velocity are shown in Fig. 10. The Δ HTE increases with both velocities and the maximum value is reached at roughly 10%.

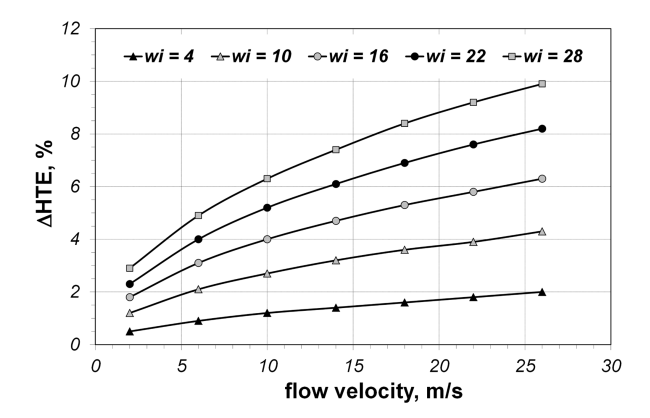


Fig. 10. ΔHTE values versus flue gas and air velocities

The results obtained for the other models are much more similar, particularly for the models M1, M2 and M6 where the maximum difference between the results is just 0.5%. That result allows us to conclude that those models are pretty similar. On the other hand, the results of the models M3, M4 and M5 differ from the averaged result of the models M1, M2 and M6 by a maximum of 1.2%, 3.4% and 6.2%, respectively. It can thus be concluded that the discrepancies of obtained values of the HTE parameter are pretty minor and acceptable for all the models considered, and each of the presented models can be used to determine the effectiveness of the heat transfer in the cross-flow heat exchanger. However, bearing in mind the extension of the model, it may be concluded that the optimal solution is the model M6, where the value of the Nusselt number is just dependent on the Reynolds number. The application of that model does not require any information on the Prandtl number.

4. Conclusions

Based on the performed calculations, it was shown that the effectiveness of the heat transfer for a cross-flow heat exchanger with staggered tube banks varies from 0.3 to 0.47, depending on the flow velocity. The maximum discrepancy between the results obtained for the analyzed models was 10%, however, the application of three models resulted in discrepancies smaller than 0.5%. The obtained results indicate that, for the analyzed heat exchanger case, one can apply the simplest model, where only the Reynolds number is the parameter used for the calculation of the HTE values. The obtained results show that the choice of the convection model for the tube bundle can, in some cases, influence the analysis of the heat exchanger's performance using the NTU method.

References

- [1] V.N. Nageswara Rao and B. Ravi Sankar. Heat transfer and friction factor investigations of CuO nanofluid flow in a double pipe U-bend heat exchanger. *Materials Today: Proceedings*, 18:207–218, 2019. doi: 10.1016/j.matpr.2019.06.294.
- [2] M. Omidi, M. Farhadi, and M. Jafari. A comprehensive review on double pipe heat exchangers. *Applied Thermal Engineering*, 110:1075–1090, 2017. doi: 10.1016/j.applthermal eng.2016.09.027.
- [3] W.G. Wheatley, R. Branco, J.A.F.O. Correia, R.F. Martins, W. Macek, Z. Marciniak, and M. Szala. Influence of heat treatment temperature on fatigue toughness in medium-carbon high-strength steels. In G. Lesiuk et al. (editors): *Fatigue and Fracture of Materials and Structures, Structural Integrity*, vol. 24, pages 283–289. Springer, Cham, 2022. doi: 10.1007/978-3-030-97822-8_33.
- [4] B. Skowrońska, T. Chmielewski, M. Baranowski, M. Kulczyk, and J. Skiba. Friction weldability of ultrafine-grained titanium grade 2. *Journal of Advanced Joining Processes*, 10:100246, 2024. doi: 10.1016/j.jajp.2024.100246.
- [5] H. Li et al. A comprehensive review of heat transfer enhancement and flow characteristics in the concentric pipe heat exchanger. *Powder Technology*, 397:117037, 2022. doi: 10.1016/j.powtec.2021.117037.
- [6] M.J. Alshukri, A.K. Hussein, A.E. Eidan, and Amma I. Alsabery. A review on applications and techniques of improving the performance of heat pipe-solar collector systems. *Solar Energy*, 236:417–433, 2022. doi: 10.1016/j.solener.2022.03.022.
- [7] M. Ding, C. Liu, and Z. Rao. Experimental investigation on heat transfer characteristic of TiO₂-H₂O nanofluid in microchannel for thermal energy storage. *Applied Thermal Engineering*, 160:114024, 2019. doi: 10.1016/j.applthermaleng.2019.114024.
- [8] T. Węgrzyn, K. Gołombek, B. Szczucka-Lasota, T. Szymczak, B. Łazarz, and K. Lukaszkowicz. Docol 1300M micro-jet-cooled weld in microstructural and mechanical approaches concerning applications at cyclic loading. *Materials*, 17(12):2934, 2024. doi: 10.3390/ma17122934.
- [9] P.C. Mukesh Kumar, K. Palanisamy, and V. Vijayan. Stability analysis of heat transfer hybrid/water nanofluids. *Materials Today: Proceedings*, 21:708–712, 2020. doi: 10.1016/j.matpr. 2019.06.743.
- [10] E.C. Okonkwo, I. Wole-Osho, I.W. Almanassra, Y.M. Abdullatif, and T. Al-Ansari. An updated review of nanofluids in various heat transfer devices. *Journal of Thermal Analysis and Calorimetry*, 145:2817–2872, 2021. doi: 10.1007/s10973-020-09760-2.

- [11] T. Sałaciński, J. Chrzanowski, and T. Chmielewski. Statistical process control using control charts with variable parameters. *Processes*, 11(9):2744, 2023. doi: 10.3390/pr11092744.
- [12] P. Podulka, W. Macek, M. Szala, A. Kubit, K.C. Das, and G. Królczyk. Evaluation of high-frequency roughness measurement errors for composite and ceramic surfaces after machining. *Journal of Manufacturing Processes*, 121:150–171, 2024. doi: 10.1016/j.jmapro.2024.05.032.
- [13] J. Sarkar, P. Ghosh, and A. Adil. A review on hybrid nanofluids: Recent research, development and applications. *Renewable and Sustainable Energy Reviews*, 43:164–177, 2015. doi: 10.1016/j.rser.2014.11.023.
- [14] A.Z. Sahin, M.A. Uddin, B.S. Yilbas, and A. Al-Sharafi. Performance enhancement of solar energy systems using nanofluids: An updated review. *Renewable Energy*, 145:1126–1148, 2020. doi: 10.1016/j.renene.2019.06.108.
- [15] M. Szala, L. Łatka, M. Awtoniuk, M. Winnicki, and M. Michalak. Neural modelling of APS thermal spray process parameters for optimizing the hardness, porosity and cavitation erosion resistance of Al₂O₃-13 wt% TiO₂ coatings. *Processes*, 8(12):1544, 2020. doi: 10.3390/pr8121544.
- [16] B. Szczucka-Lasota, T. Węgrzyn, and A. Jurek. Formation of oxides and sulfides during the welding process of S700MC steel by using new electrodes wires. *Materials*, 17(12):2974, 2024. doi: 10.3390/ma17122974.
- [17] M.E. Zayed, J. Zhao, Y. Du, A.E. Kabbel, and S.M. Shalaby. Factors affecting the thermal performance of the flat plate solar collector using nanofluids: A review. *Solar Energy*, 182:382–396, 2019. doi: 10.1016/j.solener.2019.02.054.
- [18] J. Singh, H. Vasudev, M. Szala, and H.S. Gill. Neural computing for erosion assessment in Al-20TiO₂ HVOF thermal spray coating. *International Journal on Interactive Design and Manufacturing*, 18:2321–2332, 2024. doi: 10.1007/s12008-023-01372-y.
- [19] B. Skowrońska, B. Szulc, R. Morek, M. Baranowski, and T.M. Chmielewski. Selected properties of X120Mn12 steel welded joints by means of the plasma-MAG hybrid method. *Proceedings of the Institution of Mechanical Engineers, Part L: Journal of Materials: Design and Applications*, 238(12):2460–2470, 2024. doi: 10.1177/14644207241256113.
- [20] B. Skowrońska, T. Chmielewski, D. Golański, and J. Szulc. Weldability of S700MC steel welded with the hybrid plasma + MAG method. *Manufacturing Review*, 7:4, 2020. doi: 10.1051/mfreview/2020001.
- [21] R.K. Shah and D.P. Sekulić. *Fundamentals of Heat Exchanger Design*, 1st edition, John Wiley and Sons, 2003.
- [22] T. Kuppan. Heat Exchanger Design Handbook, 2nd edition. CRC Press, Boca Raton, 2013.
- [23] A. Bejan and A.D. Kraus (editors). *Heat Transfer Handbook*. John Wiley and Sons, New York, 2003.
- [24] S. Kakaç and H. Liu. Heat Exchangers: Selection, Rating, and Thermal Design, 2nd edition. CRC Press, Boca Raton, 2002.
- [25] W.M. Kays and A.L. London. Compact Heat Exchangers, 3rd edition. Krieger Pub. Co., Malabar, 1998.
- [26] E. Kostowski. *Heat Flow*, 2nd edition. Silesian University of Technology Publishing House, Gliwice, 2006. (in Polish)
- [27] G.F. Naterer. Heat Transfer in Single and Multiphase Systems, 1st edition. CRC Press, 2002.
- [28] E. Kalinowski. *Heat Transfer and Heat Exchangers*. Publishing House of the Wrocław University of Science and Technology, Wrocław, 1995. (in Polish)
- [29] K. Raźnjević. Handbook of Thermodynamic Tables with Charts. 2nd edition, Hemisphere Publishing Co., 1976.
- [30] Y.A. Çengel. Heat and Mass Transfer: A Practical Approach, 3rd edition, McGraw-Hill, 2007.
- [31] S. Wiśniewski and T. Wiśniewski. *Heat Exchange*. Scientific and Technical Publishing House, Warsaw, 2012. (in Polish)